

## Easy plane anisotropy in $\text{Bi}_2\text{CuO}_4$

This article has been downloaded from IOPscience. Please scroll down to see the full text article.

2010 J. Phys.: Condens. Matter 22 026006

(<http://iopscience.iop.org/0953-8984/22/2/026006>)

[The Table of Contents](#) and [more related content](#) is available

Download details:

IP Address: 161.53.9.221

The article was downloaded on 15/12/2009 at 09:08

Please note that [terms and conditions apply](#).

# Easy plane anisotropy in $\text{Bi}_2\text{CuO}_4$

Mirta Herak<sup>1,3</sup>, Marko Miljak<sup>1</sup>, Guy Dhalenne<sup>2</sup> and Alexandre Revcolevschi<sup>2</sup>

<sup>1</sup> Institut za fiziku, Bijenička c. 46, HR-10000 Zagreb, Croatia

<sup>2</sup> Laboratoire de Physico-Chimie de l'Etat Solide, Université de Paris Sud, UMR8182, 91405 Orsay, France

E-mail: [mirta@ifs.hr](mailto:mirta@ifs.hr)

Received 6 October 2009, in final form 16 November 2009

Published 14 December 2009

Online at [stacks.iop.org/JPhysCM/22/026006](http://stacks.iop.org/JPhysCM/22/026006)

## Abstract

dc magnetic susceptibility measurements and the torque magnetometry were used to experimentally probe the symmetry of the antiferromagnetically (AFM) ordered state of  $\text{Bi}_2\text{CuO}_4$ . A phenomenological approach to the anisotropy energy is used to model the angular dependence of torque for easy axis and easy plane anisotropy. Comparison of these results with the experimentally obtained curves leads to the conclusion that the antiferromagnetically ordered state in  $\text{Bi}_2\text{CuO}_4$  has an easy plane anisotropy with the  $c$  plane as an easy plane. The estimated value of the critical field for the spin-flop in the easy plane is  $H_c \approx 15\text{--}20$  kOe giving the easy plane anisotropy energy constant  $K_{22} \approx 27\text{--}47 \times 10^3$  erg mol<sup>-1</sup>. The resulting antiferromagnetic structure contains two equally populated mutually perpendicular AFM domains in zero magnetic field.

## 1. Introduction

The magnetism of copper oxides is usually well described by the isotropic Heisenberg Hamiltonian. The reason is that the magnetic  $\text{Cu}^{2+}$  ion in a  $3d^9$  configuration in these compounds is usually surrounded by a distorted octahedron or a square of oxygen ions which quenches the orbital angular momentum of the unpaired electron of the copper ion. This leaves only the spin of the unpaired electron  $S = 1/2$  to contribute to the magnetic moment of the ion, thus eliminating the single ion anisotropy. The influence of the spin-orbit coupling is taken into account through the electron  $g$  factor, which is then larger than the free electron value of  $g = 2.0023$  and is usually anisotropic. However, many of these compounds exhibit a long range antiferromagnetic ordering at low temperatures, with spins pointing in a specific direction in space signifying that there is a finite, if small, magnetic anisotropy in these systems. Microscopically, this anisotropy is described by the anisotropic interactions between the spins i.e. by the anisotropic exchange Hamiltonian. For the layered lattices with tetragonal symmetry found in many copper oxides, it was shown that it is necessary to take into account Coulomb exchange terms between different orbitals to obtain anisotropy, and in the case of lower symmetry, the Hamiltonian is anisotropic even when that is neglected [1–3].

For tetragonal symmetry, easy plane anisotropy is obtained. To explain the direction of the spins within the easy plane observed in some systems it was shown that the influence of the quantum zero point fluctuations must be taken into account ([3] and references within). The anisotropy of the exchange in spin  $S = 1/2$  systems is usually very small,  $\approx 1\%$  of the isotropic exchange. It is sometimes difficult to experimentally determine the anisotropy of these systems and, often, different experiments and theoretical analysis lead to different conclusions. Such is the case of the title compound,  $\text{Bi}_2\text{CuO}_4$ .

The tetragonal crystal structure of  $\text{Bi}_2\text{CuO}_4$  belongs to the space group  $P4/ncc$  with unit cell parameters  $a = b = 8.5039$  Å and  $c = 5.8202$  Å [4].  $\text{CuO}_4$  square units are stacked along the  $c$  axis in a staggered manner, see figure 1. Each square is isolated so there is no Cu–O–Cu superexchange path as in many other cuprates. In this compound superexchange is realized through Cu–O–Bi–O–Cu paths [4–9]. Bismuth ions  $\text{Bi}^{3+}$  have a  $6s^2$  configuration which constitutes a lone electron pair E. Each  $\text{Bi}^{3+}$  is surrounded by four oxygen ions which make a  $\text{BiO}_4\text{E}$  trigonal bipyramid, where one oxygen is replaced by a lone pair E. The shortest Cu–Cu distance is along the  $c$  axis,  $d(\text{Cu–Cu}) = 2.9$  Å. The first report of the magnetic properties of this system classified it as a low dimensional antiferromagnet due to a maximum in the temperature dependence of the magnetic susceptibility [10]. However, neutron powder scattering [4, 6, 11] and single

<sup>3</sup> Author to whom any correspondence should be addressed.

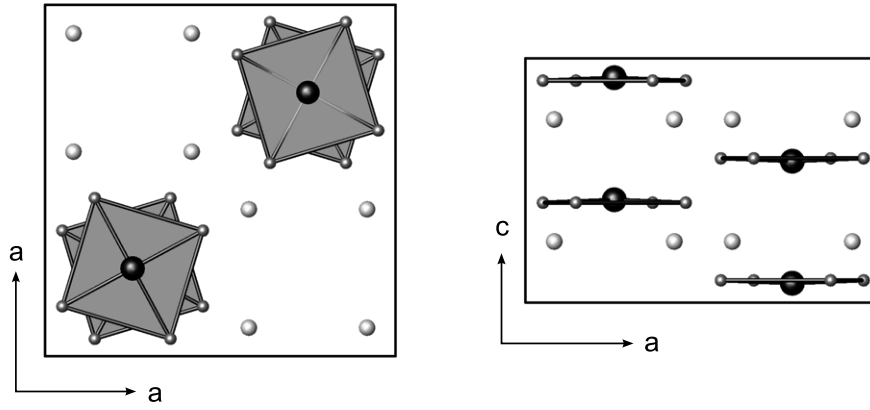


**Figure 1.** Crystal structure of  $\text{Bi}_2\text{CuO}_4$ .  $\text{CuO}_4$  square units are shown with large black spheres in the middle as Cu atoms and small spheres as O atoms. Grey spheres outside of the  $\text{CuO}_4$  units represent Bi atoms.

crystal neutron measurements [12] showed that  $\text{Bi}_2\text{CuO}_4$  orders antiferromagnetically at  $T_N \approx 42$  K with the vector of the propagation of magnetic order  $\mathbf{k} = (0, 0, 1)$ . The direction of the magnetic moments in the ordered state could not be determined from the neutron powder measurements and the  $c$  axis direction was assumed. Neutron measurements on a single crystal suggest that the magnetic moments are in the  $c$  plane [12]. The dependence of the magnetic susceptibility on the magnetic field in the  $c$  plane supports this and also suggests that the  $c$  plane is an easy plane [12]. On the other hand, the results of Raman scattering can be explained within an interacting spin wave theory if the easy axis anisotropy is assumed with the  $c$  axis as an easy axis [8]. High frequency AFMR measurements support the easy plane type of anisotropy in  $\text{Bi}_2\text{CuO}_4$  with the  $c$  plane as the easy plane [13] and also the angular dependence of the resonant field in AFMR [14]. The widening of the linewidth obtained from AFMR was explained by the small anisotropy of exchange of  $\approx 1\%$  [15]. Theoretical work favours the easy axis anisotropy. Cluster calculations of the anisotropy energy caused by the dipole-dipole interaction and the anisotropic exchange interaction give an easy axis anisotropy with the  $c$  axis as an easy axis [16]. Band structure calculations within the local spin density approximation (LSDA +  $U$ ) were used recently to obtain the leading exchange interactions and the spin anisotropy in  $\text{Bi}_2\text{CuO}_4$  [17]. These calculations also give the easy axis anisotropy with the spins parallel to the tetragonal  $c$  axis.

The issue of the type of the magnetic anisotropy in the antiferromagnetically ordered state in  $\text{Bi}_2\text{CuO}_4$  is still under debate. Torque magnetometry is one of the experimental methods that can probe the macroscopic anisotropy of the system. In this work the results of this experimental technique are used to probe the anisotropy in the title compound. Following Néel's description of the spin-flop transition [18], the phenomenological approach to the magnetic anisotropy is used to calculate the angular dependence of the torque for an easy axis type of anisotropy and an easy plane type. These results are compared with the results of the measurements.

The paper is organized as follows. In section 2 the experimental techniques used for the measurements are briefly described. In section 3 the results of the measurements are

given. In section 4.1 the phenomenological approach to the easy axis anisotropy is introduced and the angular dependence of the torque for this type of anisotropy is calculated. In section 4.2 the same is done for the easy plane anisotropy. The results are compared with those of experiment. A possible explanation for the observed results and the conclusion are given in section 5.

## 2. Experimental details

The single crystal sample used in this experiment was synthesized using a floating zone method in a mirror furnace [19]. The resulting sample was cylindrical in shape, with the tetragonal  $c$  axis perpendicular to the base of the cylinder, and several centimetres long. All measurements were performed on pieces of this sample. Powder for susceptibility measurements was obtained by crushing a piece of the single crystal sample.

The dc magnetic susceptibility of single crystal and powder  $\text{Bi}_2\text{CuO}_4$  was measured with a home-made Faraday apparatus [20] in fields up to 9 kOe. The temperature dependence of the susceptibility was measured in the 2–330 K temperature range. The powder was put in a specially designed sample holder made of ultrapure quartz. The small contribution from the sample holder was subtracted from the measured susceptibility. The mass of the sample was  $m = 23$  mg. For this mass the resolution of the measured susceptibility in 9 kOe is limited to  $\delta(\chi_m) \approx 10^{-9}$  emu g $^{-1}$ , and for  $\text{Bi}_2\text{CuO}_4$  with molar mass  $M_{\text{mol}} = 545$  g mol $^{-1}$ , this gives  $\delta(\chi_{\text{mol}}) \approx 10^{-7}$  emu mol $^{-1}$ .

The torque was measured on a piece of the sample taken from the same large single crystal. A home-made torque magnetometer was used. The applied fields ranged up to 8.4 kOe and the temperature range from 2 to 330 K. The sample holder is also made from ultrapure quartz. The contribution from the sample holder was negligible ( $<1\%$ ) compared to the signal of the sample. The samples used had masses  $m = 1.23$  and 4.44 mg which limits the resolution of the apparatus to  $\delta(\Delta\chi) \approx 5 \times 10^{-7}$  emu mol $^{-1}$  in a field of 8.4 kOe.

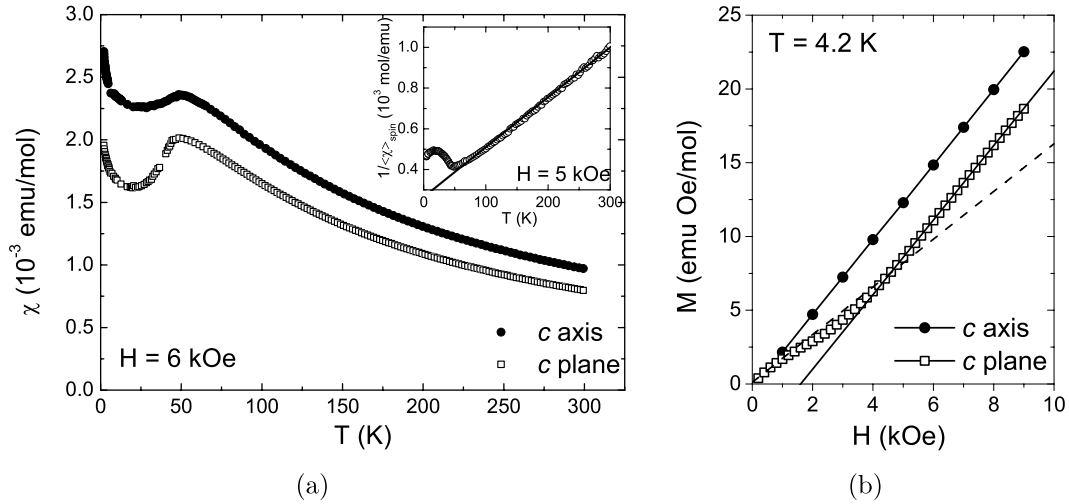


**Figure 2.** (a) Magnetic susceptibility of  $\text{Bi}_2\text{CuO}_4$  measured with the field along the  $c$  axis and in the  $c$  plane. Inset: Curie–Weiss plot of average spin susceptibility. (b) Magnetization  $M$  versus magnetic field  $H$  at  $T = 4.2$  K measured with the field applied along the  $c$  axis and in the  $c$  plane. The dashed line and solid line represent linear fits to the data in the field ranges 0–1 kOe and 6–9 kOe, respectively.

### 3. Results

The temperature dependence of the single crystal magnetic susceptibility of  $\text{Bi}_2\text{CuO}_4$  is shown in figure 2(a). The susceptibility was measured with a magnetic field applied along the  $c$  axis and in the  $c$  plane. Powder susceptibility,  $\langle\chi\rangle$ , was also measured. Average spin susceptibility,  $\langle\chi\rangle_{\text{spin}}$ , was obtained by subtracting the temperature independent diamagnetic contribution,  $\chi_{\text{dia}} = -1.09 \times 10^{-4} \text{ emu mol}^{-1}$ , and the average Van Vleck paramagnetic contribution [12],  $\chi_{\text{VV}} = 0.44 \times 10^{-4} \text{ emu mol}^{-1}$ . The spin susceptibility obeys the Curie–Weiss (CW) law at high temperatures, as can be seen in the inset of figure 2(a). The values of the Curie constant,  $C$ , and CW temperature,  $\Theta$ , obtained from the fit to the CW law are  $C = (0.408 \pm 0.007) \text{ emu K mol}^{-1}$  and  $\Theta = (-100 \pm 5) \text{ K}$  respectively. The  $g$  value calculated from the Curie constant, assuming one Cu atom per mole is  $\langle g \rangle = 2.09$ , in agreement with the value obtained from the ESR measurements [11, 15]. A negative CW temperature  $\Theta$  signifies antiferromagnetic interactions between the magnetic moments. The susceptibility for both field directions displays a sharp maximum at  $T_{\text{max}} \approx 50 \text{ K}$  and at  $T_{\text{N}} \approx 42 \text{ K}$  displays a kink and then decreases rapidly upon decreasing temperature. The decrease is more pronounced in the  $c$  plane. Both measured susceptibilities reach a minimum, but at different temperatures, and then start to increase with a decrease of the temperature. This is similar to the results observed by Yamada *et al* [12]. Their results show that the temperature and the value of the minimum of the susceptibility in the AFM state in the  $c$  plane increase as the field increases. These authors attribute this type of behaviour to an easy plane anisotropy in the  $c$  plane and the reorientation of the magnetic domains in  $\text{Bi}_2\text{CuO}_4$ . Figure 2(b) shows the field dependence of the magnetization measured on a single crystal at  $T = 4.2 \text{ K}$  with the field applied along the  $c$  axis and in the  $c$  plane. The magnetization is linear with field along the  $c$  axis, up to the highest applied field of 9 kOe. For a field applied in the  $c$  plane, the magnetization is linear in small fields

(<1 kOe) and in fields from  $\approx 5$  to 9 kOe. For field values 1–5 kOe the field dependence is not linear. A linear fit of the low field data (<1 kOe) is presented with a dashed line in figure 2(b) and a linear fit of the data in the field range 6–9 kOe with a solid line. Low field data have a smaller slope than the high field data and have no intercept, whereas high field data have a slope similar to the one for the  $c$  axis but also a nonphysical negative intercept. This is similar to what is observed for polycrystalline samples, where each grain is anisotropic and rotates when the field is applied to align the largest component of the magnetization with the field. If the response was linear in the whole field range, the magnetization would follow the dashed linear curve shown in figure 2(b). Instead, the magnetization has a larger value in high fields, which means that  $\chi_{\text{high field}} > \chi_{\text{low field}}$ .

The magnetic torque  $\Gamma$  is given by the following expression:

$$\Gamma = V \mathbf{M} \times \mathbf{B}, \quad (3.1)$$

where  $V$  is the volume of the sample,  $\mathbf{M}$  is the magnetization, and  $\mathbf{B}$  is the magnetic field in the sample. In case of a paramagnet the value of the induced magnetization  $M$  is very small and the effects of the demagnetization can be ignored so  $\mathbf{B}$  can be replaced by the applied magnetic field  $\mathbf{H}$ . For an anisotropic paramagnet a component of the induced magnetization  $M_i$  is given by

$$M_i = \sum_j \chi_{ij} H_j, \quad i, j = x, y, z, \quad (3.2)$$

where  $\chi_{ij}$  are the components of the susceptibility tensor  $\hat{\chi}$ . The magnetic axes coincide with the  $x$ ,  $y$  and  $z$  axes when the tensor is diagonal in the  $(x, y, z)$  coordinate system. In the experiment the field is usually rotated in a plane, e.g. the  $xy$  plane:  $\mathbf{H} = (H \cos \phi, H \sin \phi, 0)$ ,  $\phi$  is the angle the field makes with the  $x$  axis. Only the component of the torque perpendicular to this plane,  $\Gamma_z$ , is measured. Inserting the expression for the induced magnetization, (3.2), in the

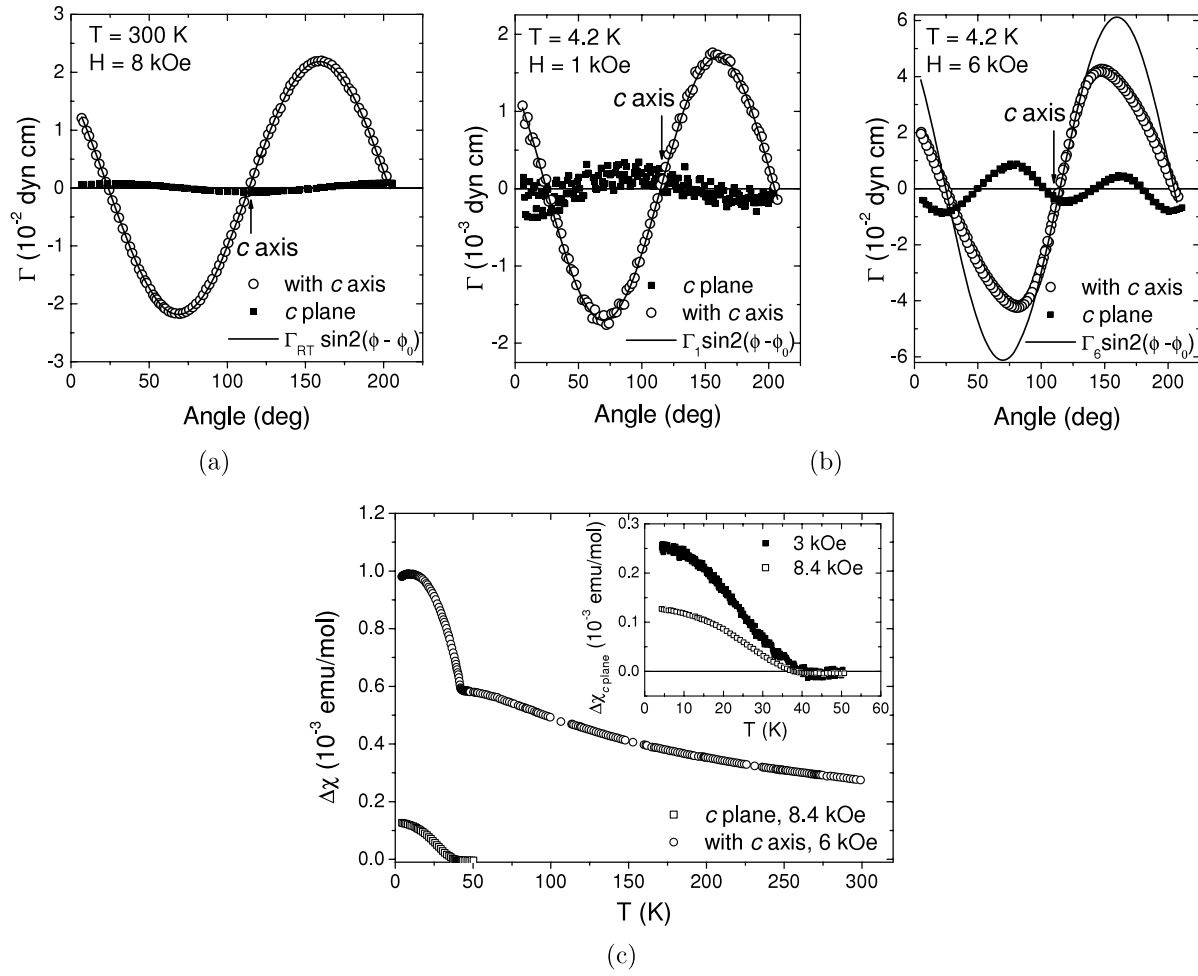


**Figure 3.** Angular dependence of the torque  $\Gamma$  in (a) the PM state and (b) the AFM state of  $\text{Bi}_2\text{CuO}_4$ . Full lines represent the paramagnetic response, expression (3.3).  $\Gamma_{RT}$  is the torque amplitude at room temperature.  $\Gamma_1$  is the torque amplitude at 4.2 K in  $H = 1$  kOe and  $\Gamma_6 = \Gamma_1 (6000/1000)^2$  is the expected amplitude in the case of the paramagnetic response. (c) Temperature dependence of the susceptibility anisotropy in  $\text{Bi}_2\text{CuO}_4$ . Inset: torque amplitude in different fields in the AFM state in the  $c$  plane.

expression for torque, (3.1), and expressing  $\chi$  in  $\text{emu mol}^{-1}$  gives the following for the measured component of the torque:

$$\Gamma_z = \frac{m}{2 M_{\text{mol}}} \Delta\chi_{xy} H^2 \sin(2\phi - 2\phi_0), \quad (3.3)$$

where  $m$  is the mass,  $M_{\text{mol}}$  is the molar mass and  $\Delta\chi_{xy}$  is the susceptibility anisotropy in the plane of the rotation of the field measured in  $\text{emu mol}^{-1}$ .  $\phi_0$  describes a phase difference resulting in the case where the magnetic axes of the sample are not aligned with the  $x$ ,  $y$  and  $z$  axes of the external coordinate system. From the measured amplitude of the torque it is possible to express the magnetic susceptibility anisotropy  $\Delta\chi_{xy} = \chi_x - \chi_y$  in the  $xy$  plane. This is possible for a paramagnet (PM) where the linear response of the magnetization to the magnetic field, given in equation (3.2), is realized. In section 4.1, it will be shown that expression (3.3) also applies to a collinear antiferromagnet (AFM) in fields much smaller than the spin-flop field. In the experiment presented here, the torque was measured in the  $c$  plane ( $\Gamma_{c \text{ plane}}$ ) and in a plane which contains the  $c$  axis and is perpendicular to the  $c$  plane ( $\Gamma_{\text{with } c \text{ axis}}$ ). The direction of the

$a$  axis in the  $c$  plane was not known. The measured angular dependence of the torque in the PM state, at 300 K, for both planes is shown in figure 3(a). The angular dependence of the torque in the PM state follows expression (3.3). The susceptibility anisotropy is calculated from the amplitude of the measured curves. For the plane which contains the  $c$  axis it is  $\Delta\chi_{\text{with } c \text{ axis}}(T = 300 \text{ K}) = 2.9 \times 10^{-4} \text{ emu mol}^{-1}$  and in the  $c$  plane  $\Delta\chi_{c \text{ plane}}(T = 300 \text{ K}) < 10^{-5} \text{ emu mol}^{-1}$ . The  $c$  plane is expected to be magnetically isotropic because of the  $g$  factor isotropy in this plane. The measured torque amplitude is indeed small, but still larger than the resolution of the experiment (in this case  $5 \times 10^{-7} \text{ emu mol}^{-1}$ ). It is very likely that the sample was not ideally mounted on the sample holder and that the  $c$  axis was slightly tilted from the position perpendicular to the plane of measurement. In that case the field did not rotate strictly in a  $c$  plane and there is a small contribution because of the tilt of the  $c$  axis which increases the measured susceptibility anisotropy. We estimate that the  $c$  axis was tilted from the perpendicular position by  $< 10^\circ$ .

In the antiferromagnetic (AFM) state, the angular dependence of the torque deviates from the paramagnetic behaviour described by expression (3.3). Figure 3(b) presents



the torque measured at  $T = 4.2$  K in  $H = 1$  and 6 kOe for both planes. In both planes a different behaviour is observed for a different applied field. The torque in a plane with the  $c$  axis has a paramagnetic behaviour in  $H = 1$  kOe, but in 6 kOe this behaviour deviates from the PM response (3.3) although the periodicity of the curve remains  $180^\circ$ . The torque in the  $c$  plane has a very small amplitude in low field, and in high field, the shape of the curve significantly deviates from the PM response (3.3). The angular dependence in the  $c$  plane resembles a sine curve with a period of  $90^\circ$  with a superimposed sine curve with a smaller amplitude and a period of  $180^\circ$ . This type of angular dependence cannot be explained in terms of a uniaxial antiferromagnet with the easy axis along the  $c$  axis, even if the spin-flop transition is considered. This will be explained in section 4 where the angular dependence of the torque will be calculated using phenomenological anisotropy energy.

The temperature dependence of the torque was measured for the two planes mentioned above. The field was applied along the direction of a maximum in the PM state, which allowed us to directly measure the susceptibility anisotropy. This is only possible for the PM state since in the AFM state the torque is not described by the expression (3.3) and  $\Delta\chi$  cannot be expressed from it, as can be seen by a deviation of the full lines (expression (3.3)) from the measured data in figure 3(b). Figure 3(c) shows the resultant temperature dependence of the susceptibility anisotropy. In the  $c$  plane, the anisotropy is practically zero in the PM state. At  $T = T_N$  the torque in the  $c$  plane displays a kink, and below  $T_N$  increases with decreasing temperature due to the increasing anisotropy of the ordered state. The amplitude below  $T_N$  in the  $c$  plane depends on the applied field (see inset of figure 3(c)). In a plane containing the  $c$  axis, the anisotropy has a temperature dependence similar to the susceptibility in the PM state. At  $T = T_N$  the torque has a kink, and below  $T_N$  increases rapidly with a temperature decrease. Both in the PM and the AFM state  $\chi_c > \chi_{c \text{ plane}}$ . At  $T \approx 11$  K, the torque reaches a maximum and then slightly decreases as temperature decreases. A uniaxial antiferromagnet in fields smaller than the spin-flop field should have a monotonous temperature dependence of the susceptibility anisotropy. This, together with the field dependence in the  $c$  plane, suggests that some kind of spin-flop or reorientation phenomenon takes place. In the next section, the phenomenological approach to the magnetic anisotropy will be used to explain the angular dependence of the torque in the AFM state of  $\text{Bi}_2\text{CuO}_4$ . This approach uses a phenomenological anisotropy energy to describe the magnetic anisotropy of the system. We will use it to calculate the angular dependence of the torque in the case of the easy axis anisotropy (which describes uniaxial antiferromagnets) and the easy plane anisotropy. The results will be compared with the measured curves.

#### 4. Phenomenological approach to magnetic anisotropy

In this section the angular dependence of the torque curves for the system with an easy axis and an easy plane

anisotropy will be calculated assuming the simplest form of the phenomenological anisotropy energy allowed by symmetry.

##### 4.1. Easy axis anisotropy

The magnetocrystalline anisotropy energy in a magnetic crystal can be described by a phenomenological expression which must be invariant under the symmetry operations of the crystal. The phenomenological expression for the easy axis anisotropy energy,  $\mathcal{F}_a$ , can be written as

$$\mathcal{F}_a = \frac{m}{M_{\text{mol}}} (K_1 \sin^2 \theta + K'_1 \sin^2 \theta \cos(2\phi)), \quad (4.1)$$

where  $m$  is the mass of the sample,  $M_{\text{mol}}$  is the molar mass,  $K_1 > 0$  and  $K'_1 > 0$  are the anisotropy constants in erg/mol units, and  $\theta$  and  $\phi$  are polar angles.  $\mathcal{F}_a$  is measured in units of ergs. The angular dependence of the easy axis anisotropy energy with  $K'_1 = 0$  and  $K_1 > 0$  is shown in figure 4(a). The  $z$  axis ( $\theta = 0, \pi$ ) is chosen for the easy axis. The  $xy$  plane is the hard plane. The effect of the finite  $K'_1$  is to describe an additional anisotropy in the hard plane.

In an applied magnetic field the total phenomenological magnetic energy is the sum of the anisotropy energy,  $\mathcal{F}_a$ , and the Zeeman energy,  $\mathcal{F}_Z$ :

$$\mathcal{F} = \mathcal{F}_a + \mathcal{F}_Z, \quad (4.2)$$

where the Zeeman energy is

$$\mathcal{F}_Z = -\frac{1}{2} \frac{m}{M_{\text{mol}}} \mathbf{H} \cdot \hat{\chi} \cdot \mathbf{H} \quad (4.3)$$

assuming a linear response of the magnetization to the magnetic field. In expression (4.3),  $\mathbf{H}$  is the magnetic field and  $\hat{\chi}$  is the magnetic susceptibility tensor with the components expressed in units of  $\text{emu mol}^{-1}$ .

A uniaxial collinear antiferromagnet has a spin axis in the direction of the easy axis in zero magnetic field. In low fields that is also true to a good approximation (as long as the value of the field is much smaller than the spin-flop field). However, as noted by Néel [18], applying high fields will in general cause the spin axis to rotate from the direction of the easy axis. The reason is that the Zeeman energy prefers the spin axis in an antiferromagnet to be perpendicular to the applied field, since  $\chi_\perp > \chi_\parallel$ , which means that  $-1/2 \chi_\perp H^2 < -1/2 \chi_\parallel H^2$ . In an isotropic antiferromagnet the spin axis will always be perpendicular to the direction of the field. In an anisotropic antiferromagnet, there is a competition of the anisotropy energy and the Zeeman energy and the spin axis will generally rotate from the easy axis direction to minimize the total energy (4.2). The new direction of the spin axis depends on the value and the direction of the applied field. Applying the critical value of the field,  $H_{\text{SF}}$ , along the easy axis direction will cause the spin-flop of the spin axis to the direction perpendicular to the easy axis.

In an applied magnetic field the spin axis rotation from the easy axis direction and the angle of rotation depends on the value and the direction of the magnetic field. This means that a different component of the susceptibility tensor is measured

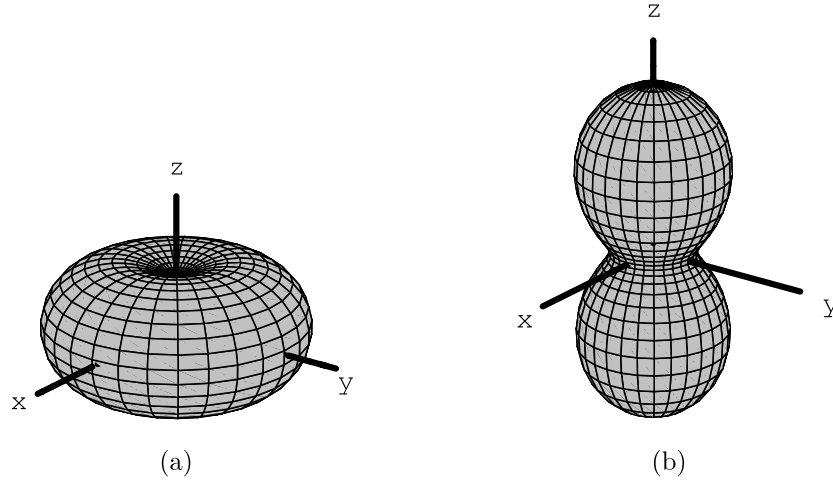


**Figure 4.** Magnetic anisotropy energy. (a) Easy axis anisotropy. (b) Easy plane anisotropy.

in different fields applied in the same direction. This rotation of the spin axis can be represented by the rotation of the susceptibility tensor. We choose the  $z$  axis as the easy axis and will describe the rotation of the spin axis with reference to this axis. The susceptibility tensor of a uniaxial antiferromagnet in zero field (and in very low fields) can be written in diagonal form:

$$\hat{\chi} (H \approx 0) = \begin{bmatrix} \chi_{\perp} & 0 & 0 \\ 0 & \chi_{\text{im}} & 0 \\ 0 & 0 & \chi_{\parallel} \end{bmatrix}, \quad (4.4)$$

where  $\chi_{\parallel}$  is the susceptibility along the easy axis,  $\chi_{\perp}$  along the hard axis and  $\chi_{\text{im}}$  along the intermediate axis. Rotation of the spin axis in higher fields is described by the rotation of the susceptibility tensor (4.4):

$$\hat{\chi} (\mathbf{H} \neq 0) = \mathbf{R}(\theta, \phi) \hat{\chi} (H \approx 0) \mathbf{R}^T(\theta, \phi), \quad (4.5)$$

where the rotation matrix is  $\mathbf{R}(\theta, \phi) = \mathbf{R}_z(\phi) \mathbf{R}_y(\theta)$ . We choose to describe the rotation of the spin axis from the easy axis as the rotation by an angle  $\theta$  around the  $y$  axis (rotation matrix  $\mathbf{R}_y$ ) and then by an angle  $\phi$  around the  $z$  axis (rotation matrix  $\mathbf{R}_z$ ). The susceptibility tensor, then, has a more general nondiagonal form:

$$\hat{\chi} (\mathbf{H} \neq 0) = \begin{bmatrix} \chi_{xx} & \chi_{xy} & \chi_{xz} \\ \chi_{yx} & \chi_{yy} & \chi_{yz} \\ \chi_{zx} & \chi_{zy} & \chi_{zz} \end{bmatrix}, \quad (4.6)$$

where  $\chi_{yx} = \chi_{xy}$ ,  $\chi_{zx} = \chi_{xz}$ ,  $\chi_{zy} = \chi_{yz}$  and the matrix elements are calculated from (4.5). The angles  $\theta$  and  $\phi$  represent the polar angles of the spin axis with respect to the easy axis. Tensor (4.6) enters expression (4.2) for the total energy. The angles  $\theta_0$  and  $\phi_0$  that the spin axis make with the easy axis in field  $\mathbf{H}$  are obtained by minimizing the total energy (4.2). The direction of the magnetic field can be described by the polar angles  $\psi$  and  $\xi$ :  $\mathbf{H} = H (\cos \psi \sin \xi, \sin \psi \sin \xi, \cos \xi)$ .  $\xi$  is the angle the magnetic field makes with the direction of the easy axis ( $z$  axis) and  $\psi$  is the angle the projection of the field on the  $xy$  plane makes with the  $x$  axis. Thus, for a given  $H$ ,  $\xi$  and  $\psi$ , the energy is minimized to give  $\theta_0$  and  $\phi_0$ .

The phenomenological approach to the spin-flop phenomenon in uniaxial antiferromagnets has been used previously to explain the reorientation effects in much more detail than will be done here (see [21] and references within). Minimization of energy (4.2) when the field is applied along the easy axis ( $\xi = 0$ ) gives two solutions for the position of the easy axis. For  $H < H_{\text{SF}}$  the spin axis remains in the direction of the easy axis and for  $H > H_{\text{SF}}$  the spin axis rotates in the direction perpendicular to the field (and easy axis). This is the spin-flop phenomenon where the spin-flop field  $H_{\text{SF}}$  is given by

$$H_{\text{SF}} = \sqrt{\frac{2 K_1}{\chi_{\perp} - \chi_{\parallel}}}. \quad (4.7)$$

The angular dependence of the torque is obtained by rotating the magnetic field in a plane of choice and measuring the component of the torque perpendicular to that plane. To calculate this in e.g. the  $xz$  plane, the magnetic field is rotated in the  $xz$  plane (see figure 5(a)). This plane is spanned by the easy axis and one hard axis. For rotation in this plane only the angle  $\xi$  changes and  $\psi = 0$ . We fix the value of the field  $H$  and choose the angle ( $\psi = 0$ ,  $\xi$ ) and then minimize the total energy (4.2) with respect to angles  $\phi$  and  $\theta$ . This gives  $(\theta_0, \phi_0)$  so the magnetic susceptibility tensor can be calculated from (4.5). Then the magnetization vector is calculated from  $\mathbf{M}(\psi, \xi) = \hat{\chi}(\theta_0, \phi_0) \mathbf{H}$ . The magnetization is expressed in units of emu Oe/mol because the magnetic susceptibility is given in emu mol<sup>-1</sup>. The torque is calculated from  $\Gamma(H, \psi, \xi) = m/M_{\text{mol}} \mathbf{M} \times \mathbf{H}$ , where  $m$  is the mass of the sample and  $M_{\text{mol}}$  is the molar mass. Only the component of the torque that is perpendicular to the plane of rotation is measured in the experiment, and in this case that is  $\Gamma_y$ . This gives one point of the curve that represents the angular dependence of the torque:  $(\xi, \Gamma_y(\psi, \xi))$ . Then the next value of  $\xi$  is chosen for the same value of the field  $H$  and the procedure is repeated. The steps used were 1°. Figure 5 shows the results of such a procedure for several values of the field  $H \leq H_{\text{SF}}$ . The following values of the parameters were used: mass  $m = 0.00128$  g (the actual mass of one of the samples used in

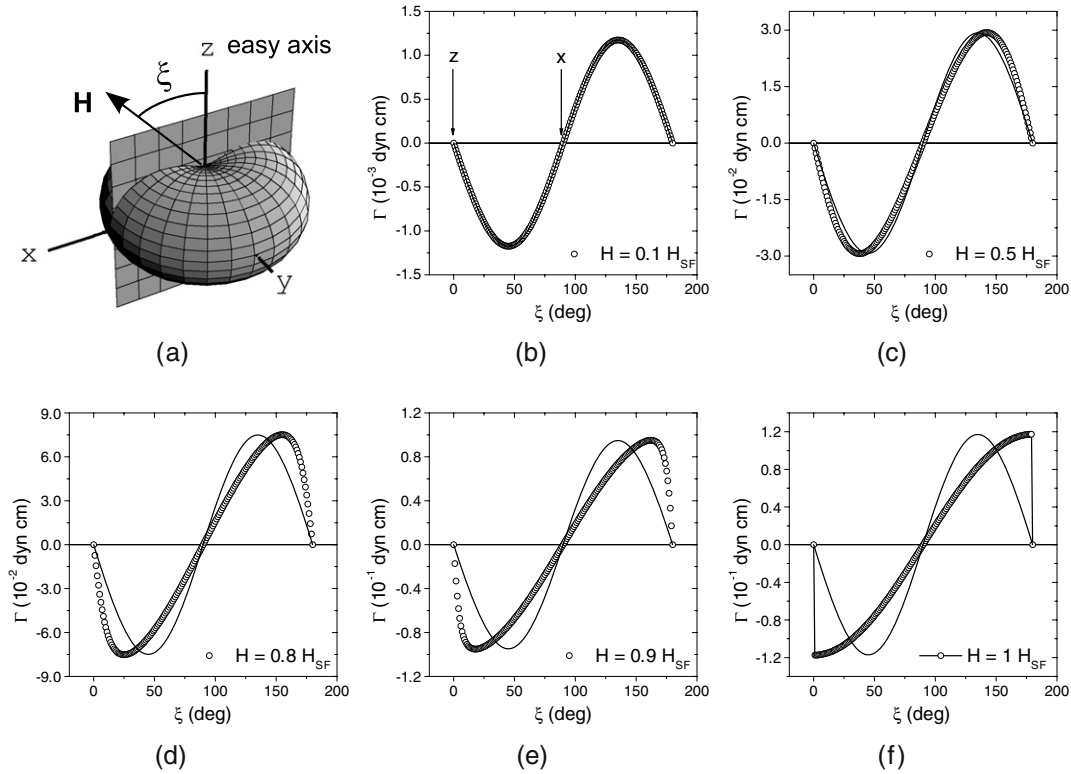


**Figure 5.** Calculated angular dependence of the torque for a system with an easy axis anisotropy for different values of the field. Figure 5(a) represents an easy axis anisotropy energy and the plane of rotation of the field,  $xz$ , for which the curves were calculated. Empty symbols represent the calculated torque and full lines the angular dependence for the paramagnetic response. The  $z$  axis is the easy axis.

experiment), molar mass  $M_{\text{mol}} = 545 \text{ g mol}^{-1}$  (molar mass of  $\text{Bi}_2\text{CuO}_4$ ), anisotropy constants  $K_1 = 5 \times 10^4 \text{ erg mol}^{-1}$ , susceptibilities  $\chi_x = \chi_y = 1.8 \times 10^{-3} \text{ emu mol}^{-1}$  (measured value of  $\chi_c$  at  $T_N$ ) and  $\chi_z = 2 \times 10^{-4} \text{ emu mol}^{-1}$  (this value was estimated). The value of the spin-flop field calculated from (4.7) is  $H_{\text{SF}} = 7906 \text{ Oe}$ .

In low fields ( $H \leq 0.2H_{\text{SF}}$ ) the angular dependence of torque for uniaxial antiferromagnet is a sine curve with a period of  $180^\circ$ , as can be seen in figure 5(b). The curve has a negative slope around the easy axis and a positive one around the hard axis direction. This type of angular dependence is also obtained for a paramagnet where the anisotropy comes from an anisotropic  $g$  factor. In the rest of the text we will refer to this type of behaviour as the paramagnetic response or the paramagnetic behaviour. In higher fields, the curves start to deviate from the paramagnetic behaviour. The slope becomes steeper in the vicinity of the easy axis, as can be seen in figures 5(c)–(e). At the spin-flop field,  $H = H_{\text{SF}}$ , the curve can be described as a sine curve with a period of  $360^\circ$  which has a sharp drop when the field is applied in the easy axis direction. The deviation of the curve from the paramagnetic response in higher fields is a consequence of the rotation of the spin axis away from the easy axis. Rotation of the field in the hard plane (perpendicular to the easy axis) in the case  $\chi_{\text{perp}} \neq \chi_{\text{im}}$  gives a paramagnetic response of the torque (a sine curve with a period of  $180^\circ$ ) for both  $H < H_{\text{SF}}$  and  $H \geq H_{\text{SF}}$ .

#### 4.2. Easy plane anisotropy

The phenomenological expression for an *easy plane anisotropy energy* can be written as

$$\mathcal{F}_a = \frac{m}{M_{\text{mol}}} (K_1 \sin^2 \theta + K_2 \sin^4 \theta + K_{22} \sin^4 \theta \cos 4\phi) \quad (4.8)$$

$$K_1 < 0, \quad K_2 < 0, \quad \text{and} \quad K_{22} < 0,$$

where  $m$  is the mass of the sample,  $M_{\text{mol}}$  is the molar mass,  $K_1$ ,  $K_2$  and  $K_{22}$  are anisotropy constants in units of  $\text{erg/mol}$  and  $\theta$  and  $\phi$  are polar angles. Expression (4.8) represents an easy plane anisotropy energy with an isotropic easy plane if  $K_{22} = 0$ . This anisotropy energy surface is shown in figure 4(b). For  $K_{22} = 0$ , any finite field in the easy plane will rotate the spin axis in the easy plane to be perpendicular to the direction of the field. When  $|K_{22}| \ll |K_1|$  the system also has an easy plane type of anisotropy with a small anisotropy in the easy plane. For small and finite  $K_{22}$ , the anisotropy energy has four minima in the easy plane, but only two nondegenerate since  $\mathcal{F}(\phi_0) = \mathcal{F}(\phi_0 + 180^\circ)$ . If  $K_{22} > 0$  the minima are at  $45^\circ$  ( $225^\circ$ ) and  $135^\circ$  ( $315^\circ$ ). If  $K_{22} < 0$  in (4.8) the minima are at  $0^\circ$  ( $180^\circ$ ) and  $90^\circ$  ( $270^\circ$ ). For finite  $K_{22}$ , there is a critical value of the field that is needed to flop the spin axis in the direction perpendicular to the field direction. We choose  $K_{22} < 0$  to model the tetragonal symmetry of the crystal structure of  $\text{Bi}_2\text{CuO}_4$  with minima represented by the axes  $x$  and  $y$ , which then correspond to the axes of high symmetry in the crystallographic  $c$  plane. For a tetragonal symmetry, these could be the crystallographic  $a$  axes, or axes in  $c$  plane



which are at  $\pm 45^\circ$  from the  $a$  axis. According to [12] these are the  $a$  axes. The axis  $z$  (hard axis) corresponds to the  $c$  axis. The easy plane is the  $xy$  plane shown in figure 4(b). Since there are minima along directions  $x$  and  $y$ , the spin axis will point in one of those directions in zero field so  $x$  and  $y$  axes can be called easy axes. The existence of the two equally probable minima results in the existence of the two perpendicular antiferromagnetic domains in zero field.

As mentioned before, finite  $K_{22}$  means there is a finite value of the magnetic field required to flop the spin axis in the easy plane. We will now find this value. We will assume that the rotation of the spin axis is confined to the easy plane, which implies  $\theta = 90^\circ$ . The vector of the magnetic field is  $\mathbf{H} = H (\cos \psi \sin \xi, \sin \psi \sin \xi, \cos \xi)$  and, if we rotate the field in the  $xy$  plane,  $\xi = 90^\circ$ . In that case, the expression for the total energy simplifies to

$$\mathcal{F} \frac{M_{\text{mol}}}{m} = K_0 + K_1 + K_2 + K_{22} \cos 4\phi + \frac{1}{2} (\chi_\perp - \chi_\parallel) H^2 \cos^2(\phi - \psi) - \frac{1}{2} \chi_\perp H^2. \quad (4.9)$$

As in the case of the spin-flop in a uniaxial antiferromagnet, we will obtain the critical field by minimizing the total energy for the field applied along the easy axis direction ( $x$  or  $y$  axes). If we choose the  $x$  axis,  $\psi = 0$ , and the minimization of (4.9) gives the following results:

$$\phi_{\min} = 0 \quad \text{if } H < H_c, \quad (4.10a)$$

$$\phi_{\max} = 0 \quad \text{if } H > H_c, \quad (4.10b)$$

$$\phi_{\min} = \pi/2, \quad \forall H, \quad (4.10c)$$

$$\phi_{\max} = \frac{1}{2} \arccos \frac{(\chi_\perp - \chi_\parallel) H^2}{16 |K_{22}|} \quad \text{if } H < H_c, \quad (4.10d)$$

where the critical field  $H_c$  is given by the expression:

$$H_c = \sqrt{\frac{16 |K_{22}|}{(\chi_\perp - \chi_\parallel)}}. \quad (4.11)$$

The anisotropy energy has two degenerate minima that remain the minima in fields  $H < H_c$  when the field is along one of the easy axes. The minimum  $\phi_0 = 90^\circ$ , which is perpendicular to the field direction, remains a minimum in all applied fields. The spin axis at  $\phi_0 = 0^\circ$  flops to  $\phi_0 = 90^\circ$  when  $H = H_c$ . This means that this system has two equally populated mutually perpendicular antiferromagnetic domains for  $H = 0$ . The repopulation of the domains in a finite field depends on the rigidity of the domain walls. If the domain walls are rigid, the domains will remain equally populated in higher fields too. If the walls are not very rigid the ratio of the volumes of different domains will vary with the applied field. In fields  $H > H_c$ , there is only one domain with the spin axis perpendicular to the direction of the field. Between the minima there is a maximum (a saddle point), (4.10c), in fields  $H < H_c$ . Applying a field  $H < H_c$  in a general direction away from the easy axis will rotate both spin axes, but in a different way. This is true for any direction of the field, not just in the easy plane. In order to calculate the torque, we assume that both domains are equally populated in zero field and in all fields for which the total energy minimization yields two nondegenerate minima. This is justified by the very narrow hysteresis of the measured curves.

The torque is calculated as in section 4 by minimizing the total energy (4.2), but with  $\mathcal{F}_a$  given by expression (4.8).

First, we calculate the angular dependence of the torque when the field is rotated in the easy plane,  $xy$ . The following values of the parameters were used for calculation:  $K_1 = -2 \times 10^6 \text{ erg mol}^{-1}$ ,  $K_2 = -2 \times 10^4 \text{ erg mol}^{-1}$ ,  $K_{22} = -2 \times 10^4 \text{ erg mol}^{-1}$ ,  $\chi_x = 1 \times 10^{-4} \text{ emu mol}^{-1}$ ,  $\chi_y = 2 \times 10^{-3} \text{ emu mol}^{-1}$  and  $\chi_z = 2.36 \times 10^{-3} \text{ emu mol}^{-1}$ ,  $m = 0.00444 \text{ g}$  (mass of the sample used for measurement) and  $M_{\text{mol}} = 545 \text{ g mol}^{-1}$ . Values of  $\chi_y$  and  $\chi_z$  are taken from the measurements of the susceptibility on the single crystal sample (shown in figure 2(a)):  $\chi_y = \chi_{\text{im}} = \chi_{c \text{ plane}}(T_N)$  and  $\chi_z = \chi_\perp = \chi_c(T_N)$ . It is not possible to measure the value of  $\chi_x = \chi_\parallel$  because of the existence of two perpendicular domains in low fields so it was chosen to be an order of magnitude smaller than  $\chi_\perp$  and  $\chi_{\text{im}}$ . In the mean field theory  $\chi_\parallel(T = 0) = 0 \text{ emu mol}^{-1}$ , but our measurements were made at  $T = 4.2 \text{ K}$  and in the case of a uniaxial antiferromagnet, a finite but small value is expected for  $\chi_\parallel$ . We want to compare the results of the calculations with the results of the experiment and so we chose a finite value for  $\chi_x$ . The chosen value of  $K_{22}$  gives the critical field  $H_c = 13 \text{ kOe}$ . Figure 6 shows the resultant curves for several different fields. Results for each domain (which has a half of the total volume) are shown in the left panel of each subfigure, and the total torque (which is the sum of the torques of both domains) is shown in the right panel. In small fields, the response within each domain is almost paramagnetic and the total torque has a very small but nonzero amplitude. The angular dependence of the total torque in small fields closely resembles a sine curve with a period of  $90^\circ$ . In higher fields (figures 6(b) and (c)) the shape of the curve deviates from the sine behaviour. The slope is negative and larger in the direction of the easy axis ( $0^\circ$  and  $90^\circ$ ) and positive and smaller at  $\pm 45^\circ$  from these directions. In field  $H = H_c$  there is only one domain and the phase of the curve is opposite to the one in smaller fields: the slope is positive around the easy axis directions and smaller than the slope  $\pm 45^\circ$  from these directions. In field  $H > H_c$  (figure 6(d)) the shape of the curve starts to resemble the shape it has in fields smaller than  $H_c$  but with two large differences: the amplitude remains constant in  $H > H_c$  and the phase is opposite to the one in lower fields. This gives a means of distinguishing whether the measurements were made in fields lower or higher than the critical field  $H_c$ . Increasing the field will of course increase the value of the induced magnetization, but in fields  $H > H_c$  the spin axes are almost perpendicular to the field and the induced magnetization is almost completely parallel to the field, and thus does not contribute to the torque. The angular dependence comes from the small perpendicular component of magnetization which is caused by the underlying constant magnetocrystalline anisotropy.

The behaviour in different fields can be understood by considering what happens to the induced magnetization when the spin axes rotate. This is shown in figure 7. When the applied field  $H < H_c$  is closer to the direction of one of the easy axes than the other, the spin axis which is along this easy axis in zero field will rotate more than the other, perpendicular, spin axis. This will cause the induced magnetization  $\mathbf{M}$  to be

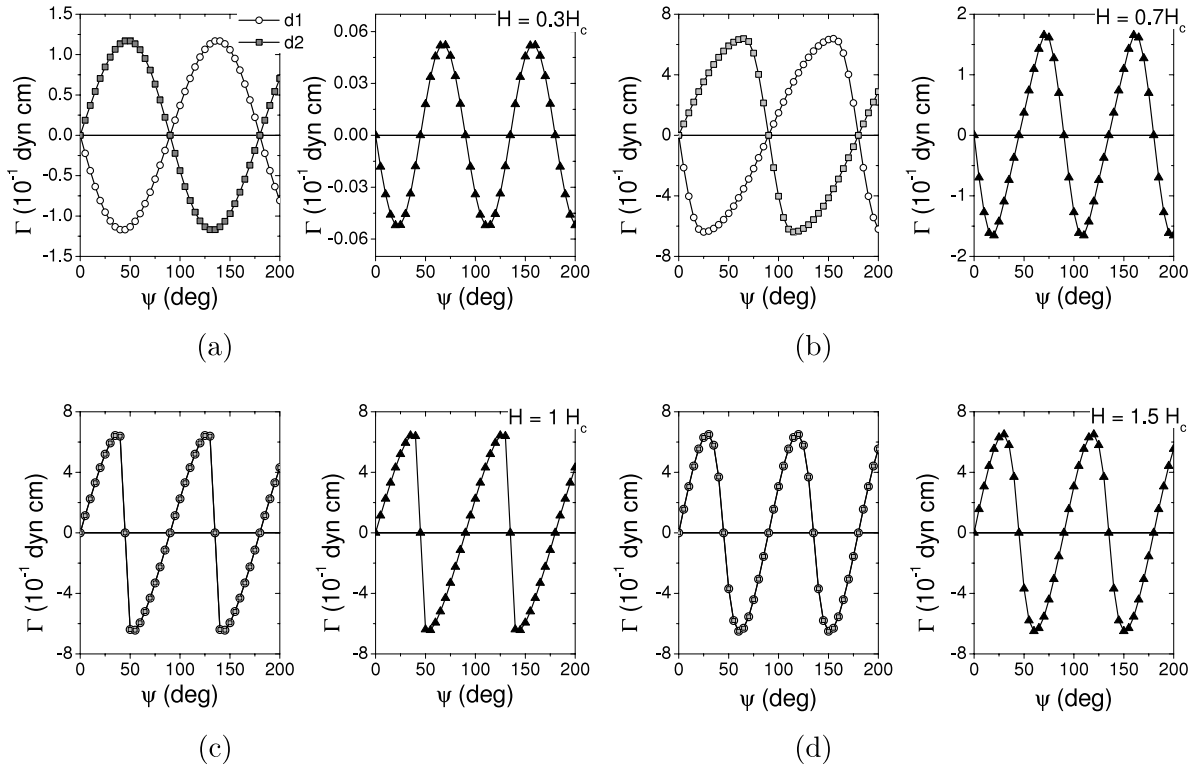


**Figure 6.** Angular dependence of torque for rotation of the field in the easy plane. Note the difference in torque scale for different fields. For each field the left panel shows calculated torques for separate domains (empty circles and full squares), and the right panel the sum of these torques, which is a total torque (full triangles). Domain 1 (d1) is the one with spin axis at  $0^\circ$  in zero field and domain 2 (d2) with spin axis at  $90^\circ$  in zero field. Parameters used in the calculation are given in the text. (a)  $H = 0.3 H_c$ ; (b)  $H = 0.7 H_c$ ; (c)  $H = 1.0 H_c$ ; (d)  $H = 1.5 H_c$ .

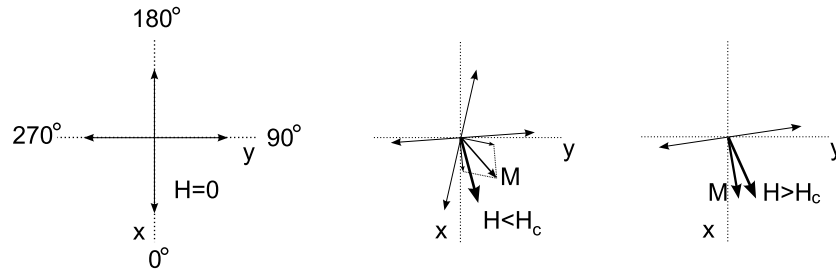


**Figure 7.** Rotation of the spin axis and induced magnetization  $\mathbf{M}$  for a magnetic field  $\mathbf{H}$  rotating in the easy plane ( $xy$  plane). Left: In zero field the spin axis are along the  $x$  and the  $y$  easy axis in the easy plane. Middle: Rotation of the spin axis in field  $H < H_c$ . Right: rotation in field  $H > H_c$ .

inclined more towards the easy axis which make a larger angle with field. So, if the field angle  $0^\circ < \psi < 45^\circ$  the resultant torque will be negative. This situation is shown in the middle panel of figure 7. When  $\psi = 45^\circ$ , the total magnetization is along the field direction and the torque is zero. When  $45^\circ < \psi < 90^\circ$ , the induced magnetization is inclined more towards the  $x$  axis and the resultant torque is positive. This is what is observed in the calculated curves, see figures 6(a) and (b). When the field is larger than the critical field  $H_c$ , there is only one domain in which the spin axes tend to be perpendicular to the direction of the field, but, due to small anisotropy, will be more inclined to the nearer easy axis. So, if  $0^\circ < \psi < 45^\circ$  the spin axis will be slightly inclined to the  $y$  easy axis and the induced magnetization will be inclined towards the  $x$  axis, which results in a positive torque. That situation is depicted in

the right panel of figure 7. For  $45^\circ < \psi < 90^\circ$  the opposite is true and the torque is negative. When  $\psi = 45^\circ$  the torque is zero because the induced magnetization is parallel to the field. This is what is observed in calculation results, see figures 6(c) and (d).

Neighbouring maxima (minima) of the calculated curves in figure 6 for the rotation of the field in the easy plane have equal values. This is not observed experimentally, as can be seen in figure 8(a). The reason for such a deviation of the measured data from the calculated results may be found in the assumption of two equally populated domains. An external anisotropy, such as a shape anisotropy, might be present which prefers one domain over the other. Another possibility is that the sample was not perfectly mounted on the sample holder and thus the plane of the rotation of the field was not an actual easy

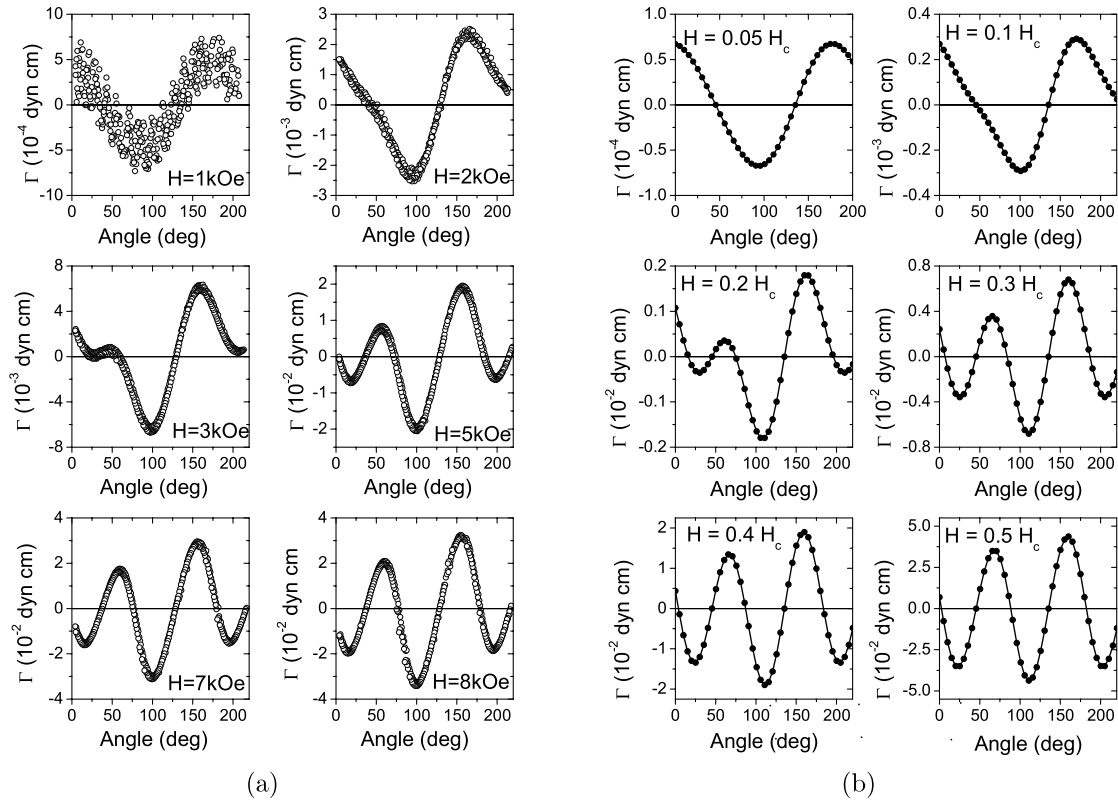


**Figure 8.** (a) Measured angular dependence of torque at  $T = 4.2$  K for a magnetic field rotating in the nominal  $c$  plane. Note the different range of torque in plots for different fields. (b) Calculated angular dependence of torque for rotation of the field in the plane shown in figure 9(a).

plane but some plane slightly tilted from the easy plane. Since there is a small but finite anisotropy in the paramagnetic state (the easy plane should be isotropic in the PM state) this seems to be the more likely cause for the disagreement between the calculated and the measured curves. To check this assumption we have calculated the angular dependence of the torque for a plane slightly tilted from the easy plane. Since the amplitude of the measured curves increases with field, we can assume that the fields applied in our experiment were smaller than the critical field  $H_c$ . From a comparison of the measured curves with the calculated ones in figures 6(a) and (b), it is possible to conclude at what angles the easy axes of the measured curves are and, from the difference in maxima, to estimate what the actual plane of rotation might be. This plane with respect to the easy plane anisotropy energy surface is shown in figure 9(a). It is a plane obtained by a  $10^\circ$  rotation of an easy plane around the  $\hat{x} + \hat{y}$  direction. The rotation of the field in this plane is described by  $H = H (\cos \psi \sin \xi, \sin \psi \sin \xi, \cos \xi)$ , where  $0^\circ < \psi < 360^\circ$  and  $\xi = 90^\circ - 10^\circ \cos(\psi - 135^\circ)$ . The measured torque is the component of the total torque perpendicular to this plane. The result of this calculation is shown in figure 8(b). The parameters used for the calculation are the same as the previously given ones. Comparing the calculation results with the measured curves, one can see that the two agree very well. The angular dependence is captured very well and even the value of the torque amplitude is quite reasonably reproduced. The choice of the anisotropy constant

$K_{22}$  was not completely random. As already mentioned, by comparing the results of the experiment with the results shown in figure 6, it was possible to conclude that the measurements were made in fields smaller than the critical field  $H_c$ . The increase of the amplitude of the measured curves started to reduce in  $H \approx 7\text{--}8$  kOe, which allowed an estimate of the critical field to be made and the starting value of  $K_{22}$  to be chosen.

The measurements performed by rotating the field in a plane containing the  $c$  axis resulted in the curves shown in figure 10. All measurements were performed in the same plane. In low fields, the curves have a paramagnetic response, i.e. can be described by sine curves with a period of  $180^\circ$ . In high fields, there is a deviation from the paramagnetic behaviour as the field rotates away from the direction of the  $c$  axis. Since the direction of the  $a$  axis in the  $c$  plane was not known and thus neither the actual plane of rotation for which the data in figure 10 were obtained, we could not calculate the equivalent torque. Instead, we chose two different planes which contained the  $c$  axis and calculated the torque curves for both of them. Figure 9(b) shows one such plane of rotation. We chose two different values for angle  $\psi$ :  $\psi = 20^\circ$  and  $45^\circ$ . Results for  $\psi = 20^\circ$  are shown in figure 11 for several different fields, and those for  $\psi = 45^\circ$  in figure 12. The figures show separate results for each domain (left panels) and the total torque, which is a sum of equal contributions from both domains (right panels). In small fields, the calculated curves

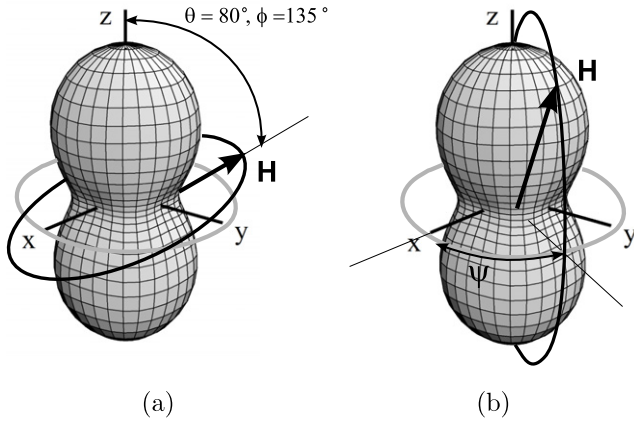


**Figure 9.** Two planes of rotation of the field with respect to the easy plane anisotropy energy surface for which the angular dependence of torque was calculated. (a) Plane of rotation which results in the torque shown in figure 8(b). (b) Plane of rotation which results in the torque shown in figures 11 and 12. The grey circle represents the easy plane.

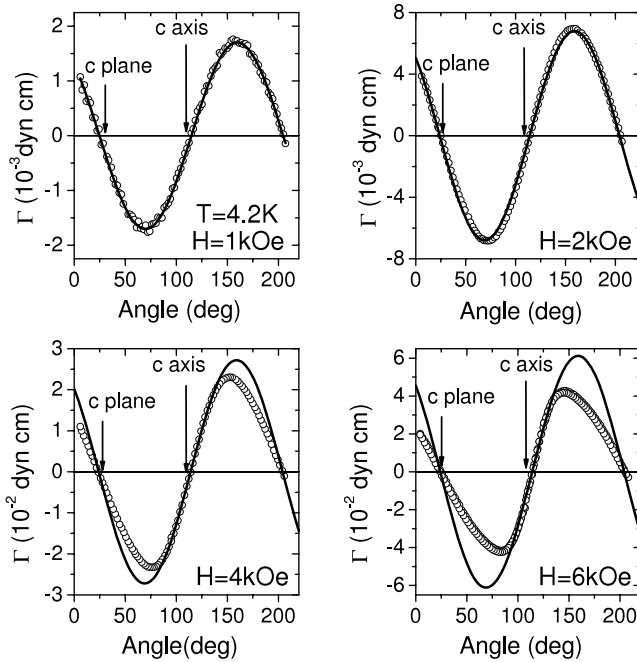


**Figure 10.** Measured angular dependence of torque in a plane which contains the  $c$  axis at  $T = 4.2$  K. All curves were measured in the same plane. Empty circles represent measured data and full lines represent sine curves with a period of  $180^\circ$  (paramagnetic response). For  $H = 1$  kOe, the curve  $\Gamma_1$  was obtained by fitting to the measured data, and for higher fields the curves were obtained by multiplying  $\Gamma_1$  with  $(H/1 \text{ kOe})^2$ , yielding the angular dependence expected in case of a paramagnetic response.

are well described by the paramagnetic response but, in higher fields, there is a deviation from the PM behaviour around the easy plane direction. This is very similar to what is observed in experiment, especially for curves calculated for  $\psi = 45^\circ$ . For  $\psi = 20^\circ$  the angular dependence of the torque is different for each domain. A spin-flop behaviour is observed in  $H = 1 H_c$  for domain 1 (domain with easy axis at  $\phi = 0^\circ$ ), but not for

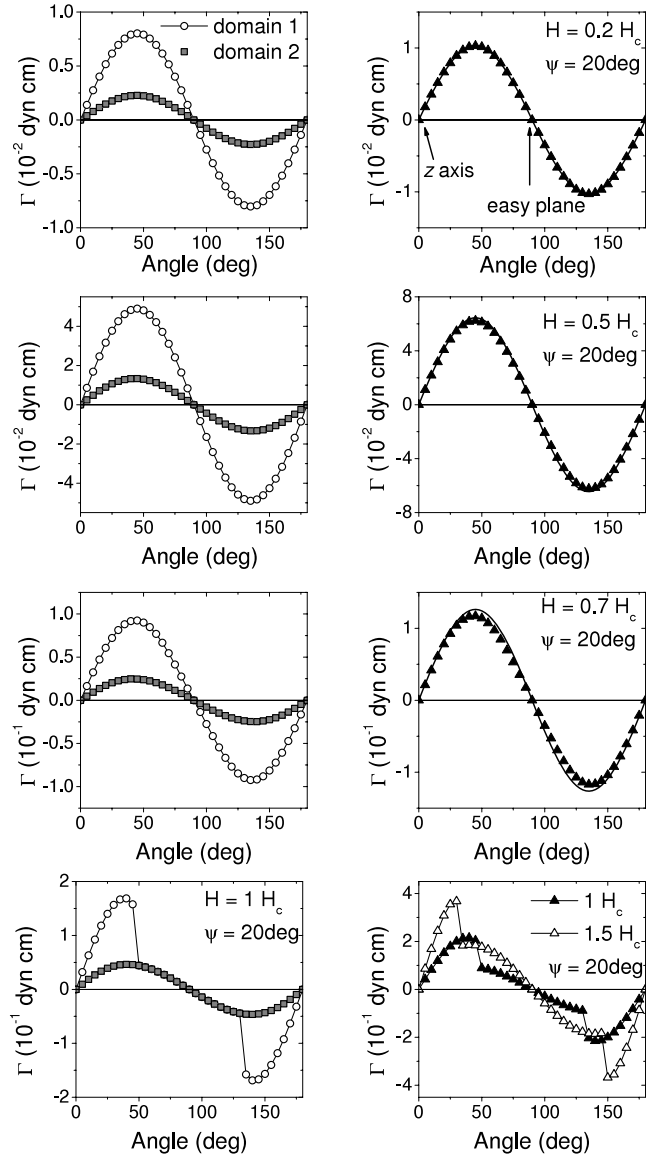


**Figure 11.** Calculated angular dependence of torque for easy plane anisotropy in the plane which contains the hard axis  $z$  with  $\psi = 20^\circ$  (see figure 9(b)). Left panels show calculated torque curves for separate domains and right panels total torque curves, which are a sum of separate contributions from the two domains. Field values are given in the right panels. Full lines represent the paramagnetic response.

domain 2 ( $\phi = 90^\circ$ ). However, it is observed for domain 2 also, but in higher fields,  $H > H_c$ . For  $\psi = 45^\circ$ , the contribution from both domains is the same since both spin axes make the same angle with the magnetic field. If the field rotates in the  $xz$  plane or the  $yz$ , plane, one of the spin axes will never undergo a spin-flop transition (the one perpendicular to the plane of rotation), and the other one will when  $H = H_c$  and in the easy plane, and in a higher field when the projection of the field on the easy plane reaches a critical value  $H_c$ . The angular dependence of the calculated torque curves in fields  $H < H_c$  describes the experimental ones rather well, especially for  $\psi = 45^\circ$ .



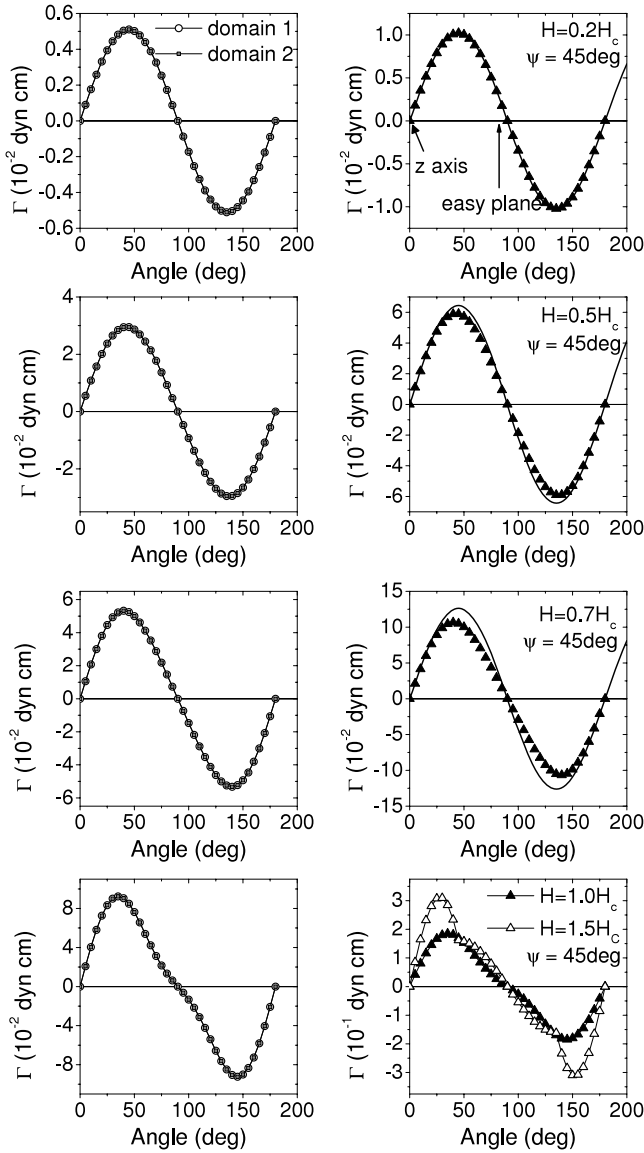


**Figure 12.** Calculated angular dependence of torque for easy plane anisotropy in the plane which contains hard axis  $z$  with  $\psi = 45^\circ$  (see figure 9(b)). Left panels show calculated torque curves for separate domains and right panels total torque curves, which are a sum of separate contributions from the two domains. Field values are given in the right panels. Full lines represent the paramagnetic response.

## 5. Discussion and conclusion

The symmetry of the antiferromagnetically ordered state of  $\text{Bi}_2\text{CuO}_4$  is still not unambiguously determined. Two different types of anisotropies are suggested from experiments and theory. One is an easy axis anisotropy with the tetragonal  $c$  axis as the easy axis. The other is an easy plane anisotropy with the  $c$  plane as an easy plane. These two anisotropies result in different spin directions in the ordered AFM state. For easy axis anisotropy, the spins are oriented in the easy axis direction (the  $c$  axis direction) and for the easy plane anisotropy the spins lie in the easy plane.

Torque magnetometry is an experimental method used for the determination of a macroscopic magnetic anisotropy

in a magnetic system. We used this experimental method to probe both the paramagnetic and the antiferromagnetic state of  $\text{Bi}_2\text{CuO}_4$ . In the paramagnetic state, the system is isotropic in the  $c$  plane, which is expected from the symmetry of the crystal structure. In the AFM ordered state, the angular dependence of torque cannot be explained within a uniaxial symmetry of the antiferromagnetic state. In order to explain the observed curves we have used the phenomenological approach to magnetic anisotropy to calculate the torque curves in different magnetic fields for both the easy axis and easy plane type of anisotropy. The simplest forms of easy axis and easy plane anisotropies allowed by symmetry are used and the deviation of the spin axis from the zero field direction (easy axis) is described by the rotation of the susceptibility tensor. The minimization of the total energy which includes the anisotropy energy and the Zeeman energy gives the new orientation of the spin axis. This rotation is described by the rotation of the susceptibility tensor from which the induced magnetization and the torque are easily calculated.

The torque was measured in the two mutually perpendicular crystallographic planes. One was the nominal  $c$  plane and the other plane contained the  $c$  axis and an unknown direction in the  $c$  plane. The torque curves calculated for the easy axis anisotropy are not observed in experiment for either of those planes. The easy plane anisotropy used in the calculations had a small in-plane anisotropy  $K_{22}$  with two mutually perpendicular energy minima, which results in the two perpendicular AFM domains in zero field. Within each domain the spins are collinear. In our calculation we assumed that the volumes of the two domains remain the same for all values of field  $H$  less than the critical value  $H_c$ . The expression for the critical field obtained is similar to the one for the spin-flop field of a uniaxial antiferromagnet. The measured curves have very small angular hysteresis, which supports rather well the assumption of equally populated domains. The curves calculated for the easy plane anisotropy describe the measured data very well, both qualitatively and quantitatively. A possible misorientation of the sample was also simulated in our calculations in order to obtain a better agreement with experiment. Due to non-ideal conditions of the experiment (possible misorientation, unknown value of  $\chi_{\parallel}$ , unknown direction of the axis  $a$  in the  $c$  plane), some of which cannot be easily overcome, it was not possible to obtain precisely the value of the critical field and, from it, the anisotropy energy. However, from the comparison of the measured and the calculated curves it is possible to estimate the anisotropy in the easy plane,  $K_{22} \approx 27\text{--}47 \times 10^3 \text{ erg mol}^{-1}$ .

The obtained experimental results are in favour of an easy plane anisotropy in  $\text{Bi}_2\text{CuO}_4$ , contrary to the theoretical results [16, 17]. In copper oxides the anisotropy is described by the anisotropic exchange. The comprehensive studies of the spin Hamiltonian of layered copper oxides with tetragonal symmetry revealed that easy plane anisotropy is obtained if both spin-orbit and Coulomb exchange interactions are included and, in case of lower symmetry, the anisotropy of the Hamiltonian always emerges [2, 3]. In order to explain the easy axis within the easy plane observed in some systems, such as the  $x$  and  $y$  axes that we assumed in our simplified



phenomenological treatment of the problem, it was shown that the quantum zero point energy fluctuations need to be taken into account [1–3]. Similar interactions might be responsible for the easy plane anisotropy in  $\text{Bi}_2\text{CuO}_4$  and further theoretical treatment is needed to show if this is the case.

To conclude, the combination of magnetic susceptibility and torque magnetometry measurements, and a phenomenological approach to anisotropy energy has allowed us to show that the anisotropy in the AFM ordered state of  $\text{Bi}_2\text{CuO}_4$  is not easy axis but easy plane anisotropy.

## Acknowledgment

The work in Zagreb was supported by the resources of the Croatian Ministry of Science, Education and Sports under Grant No. 035-0352843-2846.

## References

- [1] Yildirim T, Harris A B, Entin-Wohlman O and Aharony A 1994 *Phys. Rev. Lett.* **72** 3710
- [2] Yildirim T, Harris A B, Entin-Wohlman O and Aharony A 1994 *Phys. Rev. Lett.* **73** 2919
- [3] Yildirim T, Harris A B, Aharony A and Entin-Wohlman O 1995 *Phys. Rev. B* **52** 10239
- [4] García-Muñoz J L, Rodríguez-Carvajal J, Sapiña F, Sanchis M J, Ibáñez R and Beltrán-Porter D 1990 *J. Phys.: Condens. Matter* **2** 2205
- [5] Attfield J P 1989 *J. Phys.: Condens. Matter* **1** 7045
- [6] Troć R, Janicki J, Filatow I, Fisher P and Murasik A 1990 *J. Phys.: Condens. Matter* **2** 6989
- [7] Äin M, Dhalenne G, Guiselin O, Hennion B and Revcolevschi A 1993 *Phys. Rev. B* **47** 8167
- [8] Konstantinović M J, Konstantinović Z and Popović Z V 1996 *Phys. Rev. B* **54** 68
- [9] Gippius A A, Vasil'ev A N, Petrakovskii G A, Zalessky A V, Hoffmann W, Lüders K, Dhalenne G and Revcolevschi A 1998 *J. Magn. Magn. Mater.* **184** 358
- [10] Sreedhar K, Ganguly P and Ramasesha S 1988 *J. Phys. C: Solid State Phys.* **21** 1129
- [11] Ong E W, Kwei G H, Robinson R A, Ramakrishna B L and Von Dreele R B 1990 *Phys. Rev. B* **42** 4255
- [12] Yamada K, Takada K, Hosoya S, Watanabe Y, Endoh Y, Tomonaga N, Suzuki T, Ishigaki T, Kamiyama T, Asano H and Izumi F 1991 *J. Phys. Soc. Japan* **60** 2406
- [13] Ohta H, Ikeuchi Y, Kimura S, Okubo S, Nojiri H, Motokawa M, Hosoya S, Yamada K and Endoh Y 1998 *Physica B* **246/247** 557
- [14] Pankrats A I, Sobyenin D Y, Vorotinov A M and Petrakovski G A 1999 *Solid State Commun.* **109** 263
- [15] Ohta H, Yoshida K, Matsuya T, Nanba T, Motokawa M, Yamada K, Endoh Y and Hosoya S 1992 *J. Phys. Soc. Japan* **61** 2921
- [16] Tanaka N and Motizuki K 1998 *J. Phys. Soc. Japan* **67** 1755
- [17] Janson O, Kuzian R O, Drechsler S L and Rosner H 2007 *Phys. Rev. B* **76** 115119
- [18] Néel L 1952 *Proc. Phys. Soc. A* **65** 869
- [19] Dhalenne G, Revcolevschi A, Äin M, Hennion B, Andre G and Parette G 1991 *Cryst. Prop. Prep.* **35/36** 11
- [20] Miljak M and Cooper J R 1975 *Fizika* **7** 49
- [21] Bogdanov A N, Zhuravlev A V and Rößler U K 2007 *Phys. Rev. B* **75** 094425